Preprints, *39th Conf. on Broadcast Meteor.*, Oklahoma City, OK, Amer. Meteor. Soc., June 2011

11.1 THE TORNADIC VORTEX SIGNATURE (TVS)

RODGER A. BROWN* and VINCENT T. WOOD
NOAA/National Severe Storms Laboratory
Norman, Oklahoma

1. Introduction

During the late 1960s and early 1970s, pulsed Doppler radars began to be used to systematically study severe and tornadic thunderstorms in Massachusetts (e.g., Donaldson et al. 1966; Kraus, 1970; Donaldson 1970) and Oklahoma (e.g., Brown et al. 1971, 1973; Burgess and Brown 1973). A breakthrough in Doppler radar identification of tornadoes occurred in 1973 when the National Severe Storm Laboratory's 10–cm wavelength Doppler radar (half-power beamwidth of 0.8°) in Norman, OK, detected the presence of a Doppler velocity signature associated with the tornado that struck Union City, OK on 24 May 1973 (Burgess et al. 1975; Brown et al. 1978). The signature consisted of extreme positive and negative Doppler velocity values located at adjacent azimuths (separated by 1.0°). The signature was first detected at mid-levels in the storm and then strengthened in magnitude at all altitudes as it descended toward the ground along with the tornado. A detailed damage survey indicated that the signature coincided with the tornado track.

In order to understand the relationship between a tornado and the Doppler velocity signature, Brown et al. (1978) used the Doppler radar simulator of Zrnić and Doviak (1975) to scan idealized vortices. A Rankine vortex profile (e.g., Rankine 1882) was used to simulate the distribution of tangential velocities within the vortex, where velocity increases linearly from zero at the center of the vortex to a peak value at the core radius then decreases, changing inversely proportional to distance from the vortex center (see Fig. 3a). The radar reflectivity distribution across the vortex was assumed to be uniform; there were some indications that a weak reflectivity region is associated with the center of a tornado (e.g., Fujita 1981), but it was not apparent at that time how often it occurs or how the reflectivity is distributed relative to the core radius. The resulting simulated Doppler velocity data indicated that—for tornado core regions smaller than the radar beamwidth—Doppler velocity peaks of opposite sign are expected to occur at azimuthal locations separated by about one beamwidth regardless of distance from the radar (Fig. 1). Since it was not clear from the limited number of available observations whether all signatures aloft evolved into tornadoes touching the ground, the signature was called a Tornadic Vortex Signature (TVS; Brown et al. 1978). These simulations were in agreement with the Doppler velocity measurements associated with the Union City tornado (Fig. 2). Also, the three simulated TVS curves in the figure reveal that vortices having a variety of sizes and peak tangential velocities can produce TVS curves that have the same peak values.

With the installation of the national network of Weather Surveillance Radar–1988 Dopplers (WSR–88D) during the early and mid 1990s, the TVS began to be used operationally by the National Weather Service (NWS) to identify the presence of tornadoes (e.g., NWS WDTB 2011). The WSR–88Ds have a nominal antenna half–power beamwidth of about 0.9°. Since the simulations indicated that the peak TVS values should be about one beamwidth apart, the TVS peaks would be separated by 1.0° (adjacent azimuthal locations, commonly called "gate–to–gate shear") and occasionally by 2.0° (every other azimuthal location when one azimuthal location is close to the center of the tornado; e.g., Wood and Brown 1997).

In 2008, the azimuthal sampling interval at the lower WSR–88D elevation angles was decreased from 1.0° (legacy resolution) to 0.5° (super resolution) based on simulations and field tests (e.g., Wood et al. 2001; Brown et al. 2002, 2005). With 0.5° azimuthal data collection, one would expect the TVS peaks to be separated by about one beamwidth or 1.0° (every other azimuthal location). However, the peaks occasionally are observed to be separated by only 0.5°—contrary to the simulation results. In order to help solve this quandary, we repeated the simulations using other vortex models and other reflectivity profiles across the vortices as well as

* *Corresponding author address*: Dr. Rodger A. Brown, NOAA/National Severe Storms Laboratory, 120 David L. Boren Blvd., Norman, OK 73069; e-mail: Rodger.Brown@noaa.gov

investigating the role of effective beamwidth instead of antenna beamwidth. The findings of these new simulations are discussed in the following sections.

2. Doppler radar simulator

For the Doppler radar computations, we used a radar simulator that approximates the characteristics of the WSR–88D (e.g., Wood and Brown 1997). Since a radar antenna moves during the collection of data samples (that are used to calculate reflectivity, mean Doppler velocity, and spectrum width), the broadened data collection region is called the *effective beamwidth* (e.g., Doviak and Zrnić 1993, 193–197). The effective half–power beamwidth for a given radar can be determined from the half–power beamwidth of the antenna and the azimuthal sampling interval (e.g., Fig. 1 of Brown et al. 2002); values for the WSR–88D are listed in Table 1 along with some of the simulation results. A pulse depth of 0.25 km and an effective half–power beamwidth of 1.0^{o} were used for the simulations; since the results are normalized relative to effective beamwidth, the value chosen for the effective beamwidth is not crucial.

For simplicity, the radar scans horizontally through the vortex only at the range of the vortex center from the radar. Furthermore, we assume that the tangential velocity and reflectivity profiles across the vortex are constant with height, so that, instead of making measurements throughout the two–dimensional beam, we make measurements only in the one–dimensional horizontal direction through the center of the beam. Simulating the full width of a WSR–88D beam, we assume that the full effective beamwidth is Gaussian shaped and equal to three times the half–power effective beamwidth, which is a very good approximation of the WSR–88D beam.

A radar computes the reflectivity and mean Doppler velocity from tens of transmitted pulses. Instead, for the simulations, we computed the reflectivity and mean Doppler velocity from data at 101 evenly–distributed points across the full one–dimensional beam. A continuous distribution of mean Doppler velocity and reflectivity values were then derived by positioning the antenna at 0.001^{o} increments across the model vortex.

3. Results using four vortex models

To illustrate the influence of various vortex models on TVSs, we considered the simulation results of Wood and Brown (2011). They used a uniform reflectivity profile when investigating four vortex models: the Rankine, Burgers–Rott, Sullivan, and modified Sullivan vortex models, as shown in Fig. 3. The Rankine and Burgers–Rott models represent vortices that are associated with updrafts, while the two Sullivan models with the broader regions of zero tangential velocities at the vortex center represent vortices associated with a central downdraft surrounded by an annular updraft. Details of these vortex models are discussed by Davies–Jones (1986) and Wood and White (2011), for example. These models do not represent asymmetric vortices or vortices that contain subvortices; however such details become immaterial when the radar beam is significantly larger than the vortex.

The Wood and Brown (2011) findings are summarized in Fig. 4. The data points represent the ratios of the diameter between the positive and negative peaks of the TVS profile divided by effective beamwidth plotted as a function of effective beamwidth relative to the true vortex core diameter. For effective beamwidths greater than the vortex core diameter, the mean TVS diameter (solid curve) is between 0.8 and 1.3 times the effective beamwidth. Other than the extreme modified Sullivan vortex (the rightmost of the dots in the figure), the normalized TVS diameters are so similar for each EBW/CD ratio that one can reasonably conclude that the choice of vortex model does not affect the distance between the Doppler velocity peaks of a TVS for a given radar's effective beamwidth.

4. Results using two reflectivity profiles

With the choice of vortex model not affecting the TVS, we compared the TVSs associated with two reflectivity profiles. We chose the Burgers–Rott vortex model to represent the tornado's tangential velocity profile because it is an excellent fit to Doppler velocity measurements made by mobile Doppler radars close to tornadoes (e.g., Bluestein et al. 2007; Tanamachi et al. 2007; Kosiba and Wurman 2010). The two reflectivity profiles selected were uniform reflectivity and one with a weak–reflectivity eye at the center of the tornado. The relationship between the Burgers–Rott tangential velocity profile and the weak–reflectivity–eye profile is shown in Fig. 5. The peak reflectivity occurs at twice the tangential velocity core radius, reflecting the centrifuging of radar targets; this relationship is similar to that observed in proximity mobile Doppler radar measurements (e.g., Wurman and Gill 2000; Bluestein 2005; Wakimoto et al. 2011).

The simulation results show that there is a significant difference in the TVS diameters between the two reflectivity profiles when the effective beamwidth is up to 3.5 times larger than the tornado's core diameter (Fig. 6). With the presence of a reflectivity eye, TVS diameters are 0.7 to 0.9 times the effective beamwidth, while for uniform reflectivity the diameters are 0.9 to 1.3 times the effective beamwidth. For super–resolution WSR–88D data collection with an antenna beamwidth of 0.9^o and azimuthal sampling interval of 0.5^o, the effective beamwidth is 1.0^o (e.g., Brown et al. 2002). In this situation, where we expect peak TVS values to be 0.7^o to 0.9^o apart with minimum reflectivity at the center of a tornado, it is entirely reasonable for extreme TVS values to occur at adjacent azimuths separated by 0.5^o—consistent with WSR–88D observations. The original 1970s simulations of Brown et al. (1978), with the assumption of uniform reflectivity across the vortex, results in misleading expectations concerning super–resolution data collection at shorter distances from a radar.

At greater distances from the radar, where the effective beamwidth is larger than 3.5 times the tornado core diameter, the choice of reflectivity profile does not affect the size of the TVS, with the distance between the extreme WSR–88D Doppler velocity values being equal to 0.8 to 0.9 times the effective beamwidth (Fig. 6). For both legacy–resolution with 1.0^o azimuthal sampling interval (EBW = 1.4^o) and super–resolution with 0.5^o azimuthal sampling interval (EBW = 1.0^o), one would expect the peaks to be 1.0^o apart (Table 1).

The transition distance where EBW/CD = 3.5 occurs depends on tornado size and the azimuthal sampling interval. For example, with legacy data collection and tornadoes having core diameters ranging from 50 m to 500 m, the transition distance ranges from 7.5 km to 75 km. For super–resolution data collection, the distances range from 10.5 km to 105 km.

5. Concluding discussion

The simulations of Brown et al. (1978) indicate that the peak Doppler velocities (opposite signs) of a tornadic vortex signature should occur at about one beamwidth separation. For legacy WSR–88D data collection at 1.0^o azimuthal intervals with an effective beamwidth of 1.4^o, one expects the peak velocities to be separated by 1.0^o (adjacent azimuths) or occasionally at 2.0^o (every other azimuth). This is what is routinely observed. With the recent advent of super–resolution data collection (azimuthal increments of 0.5^o), the effective beamwidth is 1.0^o, so one would expect the peak Doppler velocity values also to be separated by 1.0^o. However, the peaks are observed to be separated by 0.5^o instead.

In order to understand this dilemma, we investigated alternative vortex models and reflectivity profiles as well as the role of effective beamwidths. Using four different vortex models having a common reflectivity profile (uniform), it was found that the choice of vortex model did not have a significant effect on the simulation results. Using two different reflectivity profiles (uniform and minimum reflectivity at the vortex center) having a common vortex model (Burgers–Rott), we found that there was a difference when the effective beamwidth was less than 3.5 times larger than the vortex's core diameter. With the presence of a reflectivity minimum (resulting from centrifuged radar targets), the simulations indicate that it is possible for the distance between the peak Doppler velocity values to be separated by 0.5^o. However, when the effective beamwidth is greater than 3.5 time the core diameter, the peak values are expected to have an azimuthal separation of 1.0^o for both legacy–resolution (one azimuthal increment) and super–resolution (two azimuthal increments) data collection. Thus, the super–resolution dilemma apparently has been resolved.

Acknowledgments. Discussions with James LaDue of the National Weather Service's Warning Decision Training Branch led to our realization that we needed to investigate the influence of various tornado vortex models and reflectivity profiles on the tornadic vortex signature.

References

Bluestein, H. B., 2005: A review of ground–based, mobile, W–band Doppler–radar observations of tornadoes and dust devils. *Dyn. Atmos. Oceans*, **40**, 163–188.

Bluestein, H. B., C. C. Weiss, M. M. French, E. M. Holthaus, and R. L. Tanamachi, 2007: The structure of tornadoes near Attica, Kansas, on 12 May 2004: High–resolution, mobile, Doppler radar observations. *Mon. Wea. Rev*., **135**, 475–506.

Brown, R. A., W. C. Bumgarner, K. C. Crawford, and D. Sirmans, 1971: Preliminary Doppler velocity measurements in a developing radar hook echo. *Bull. Amer. Meteor. Soc.*, **52**, 1186–1188.

Brown, R. A., D. W. Burgess, and K. C. Crawford, 1973: Twin tornado cyclones within a severe

thunderstorms: Single Doppler radar observations. *Weatherwise*, **26**, 63–69, 71.

Brown, R. A., L. R. Lemon, and D. W. Burgess, 1978: Tornado detection by pulsed Doppler radar. *Mon. Wea. Rev.*, **106**, 29–38.

Brown, R. A., V. T. Wood, and D. Sirmans, 2002: Improved tornado detection using simulated and actual WSR–88D data with enhanced resolution. *J. Atmos. Oceanic Technol*., **19**, 1759–1771.

Brown, R. A., B. A. Flickinger, E. Forren, D. M. Schultz, D. Sirmans, P. L. Spencer, V. T. Wood, and C. L. Ziegler, 2005: Improved detection of severe storms using experimental fine–resolution WSR–88D measurements. *Wea. Forecasting*, **20**, 3–14.

Burgess, D. W., and R. A. Brown, 1973: The structure of a severe right-moving thunderstorm: New single Doppler radar evidence. Preprints, *8th Conf. on Severe Local Storms*, Denver, CO, Amer. Meteor. Soc., 40–43.

Burgess, D. W., L. R. Lemon, and R. A. Brown, 1975: Tornado characteristics revealed by Doppler radar. *Geophys. Res. Lett*., **2**, 183–184.

Davies–Jones, R. P., 1986: Tornado dynamics. *Thunderstorm Morphology and Dynamics*, 2nd ed., E. Kessler, Ed., University of Oklahoma Press, 197–236.

Donaldson, R. J., Jr., 1970: Vortex signature recognition by a Doppler radar. *J. Appl. Meteor*., **9**, 661–670.

Donaldson, R. J., Jr., G. M. Armstrong, and D. Atlas, 1966: Doppler measurements of horizontal and vertical motions in a paired instability line. Preprints, *12th Conf. on Radar Meteor*., Norman, OK, Amer. Meteor. Soc., 392–397.

Doviak, R. J., and D. S. Zrnić, 1993: *Doppler Radar and Weather Observations*, 2nd ed., Academic Press, 562 pp.

Fujita, T. T., 1981: Tornadoes and downbursts in the context of generalized planetary scales. *J. Atmos. Sci.*, **38**, 1511–1534.

Kosiba, K., and J. Wurman, 2010: The three–dimensional axisymmetric wind field structure of the Spencer, South Dakota, 1998 tornado. *J. Atmos. Sci*., **67**, 3074–3083.

Kraus, M. J., 1970: Doppler radar investigation of flow patterns within severe thunderstorms. Preprints, *14th Radar Meteor. Conf*., Tucson, AZ, Amer. Meteor. Soc., 127–132.

NWS Warning Decision Training Branch, 2011: *Distance Learning Operations Course, Topic 5: Base and Derived Products*, http://www.wdtb.noaa.gov/courses/dloc/documentation/ DLOC_FY11_Topic5.pdf .

Rankine, W. J. M., 1882: *A Manual of Applied Physics*. 10th ed., Charles Griff and Co., 663 pp.

Tanamachi, R. L., H. B. Bluestein, W.–C. Lee, M. Bell, and A. Pazmany, 2007: Ground–based velocity track display (GBVTD) analysis of W–band Doppler radar data in a tornado near Stockton, Kansas, on 15 May 1999. *Mon. Wea. Rev*., **135**, 783–800.

Wakimoto, R. M., N. T. Atkins, and J. Wurman, 2011: The LaGrange tornado during VORTEX2. Part I: Photogrammetric analysis of the tornado combined with single–Doppler radar data. *Mon. Wea. Rev*., **139**, 2233–2258.

Wood, V. T., and R. A. Brown, 1997: Effects of radar sampling on single–Doppler velocity signatures of mesocyclones and tornadoes. *Wea. Forecasting*, **12**, 928–938.

Wood, V. T., and R. A. Brown, 2011: Simulated tornadic vortex signatures of tornado–like vortices having one– and two–celled structures. Submitted to *J. Appl. Meteor. Climatol*.

Wood, V. T., and L. W. White, 2011: A new parametric model of vortex tangential–wind profiles: Development, testing, and verification. *J. Atmos. Sci*., **68**, 990–1006.

Wood, V. T., R. A. Brown, and D. Sirmans, 2001: Technique for improving detection of WSR – 88D mesocyclone signatures by increasing angular sampling. *Wea. Forecasting*, **16**, 177–184.

Wurman, J., and S. Gill, 2000: Finescale radar observations of the Dimmitt, Texas (2 June 1995), tornado. *Mon. Wea. Rev*., **128**, 2135 – 2164.

Zrnić, D. S., and R. J. Doviak, 1975: Velocity spectra of vortices scanned by a pulse–Doppler radar. *J. Appl. Meteor*., **14**, 1531–1539.

TABLE 1. Effective beamwidth (EBW) for WSR–88D legacy– and super–resolution azimuthal data collection. Also listed are the simulation results for the ratio of TVS diameter to EBW and the azimuthal separation of TVS peak values (TVS ΔAz) based on a Burgers–Rott tangential velocity profile and a weak–reflectivity eye at the center of the vortex (Fig. 6).

WSR–88D Resolution	Azimuthal Increment	Antenna Beamwidth	Effective Beamwidth	TVS Diameter / EBW	TVS ΔAz
Legacy	1.0°	0.9°	1.4°	0.7 – 0.9	1.0°, 2.0°
Super	0.5°	0.9°	1.0°	0.7 – 0.9	0.5°, 1.0°

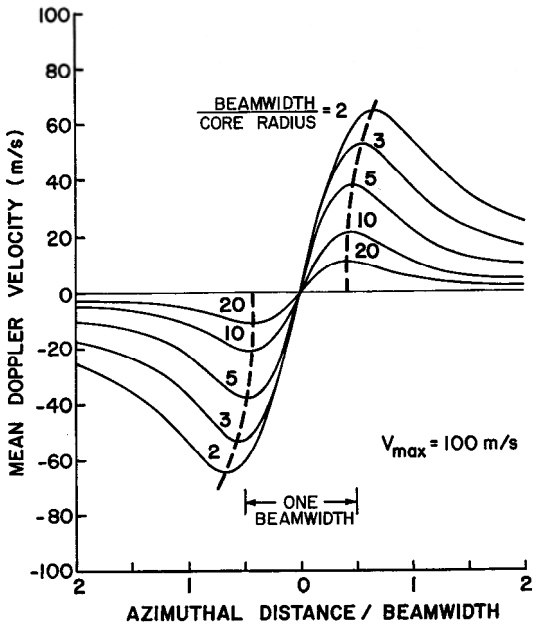

FIG. 1. Simulated azimuthal Doppler velocity profiles through the center of a tornadic vortex signature for various beamwidth to core radius ratios (representing various ranges from the radar for a given vortex). The abscissa is normalized by dividing the azimuthal distance from the vortex center by the radar's half–power beamwidth (0.8°). The maximum tangential velocity of the Rankine vortex is 100 m s^{-1}. The simulations assumed uniform reflectivity across the vortex. From Brown et al. (1978).

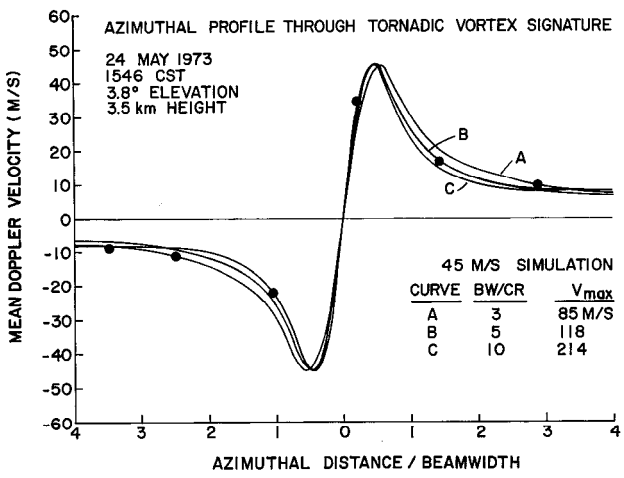

FIG. 2. Doppler velocity measurements through the center of the Union City tornado (dots) superimposed on three theoretical tornadic vortex signature curves produced by scanning a simulated radar past three Rankine vortices having distinctly different sizes (ratio of beamwidth BW to core radius CR) and peak tangential velocities (V_{max}). Reflectivity across the vortices was assumed to be uniform. From Brown et al. (1978).

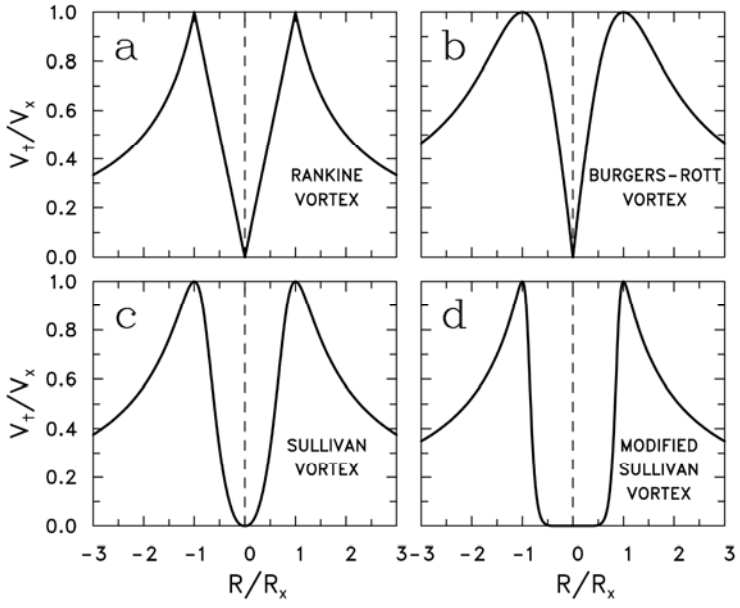

FIG. 3. Tangential velocity profiles for four idealized vortex models. The Rankine and Burgers–Rott vortices are associated with updrafts (one–celled vortices) and the two Sullivan vortices as associated with a central downdraft surrounded by an updraft (two–celled vortices); the modified Sullivan vortex represents an extreme case with an unusually wide downdraft. Tangential velocities (V_t) are normalized by the peak tangential velocity (V_x) that occurs at the core radius R_x. From Wood and Brown (2011).

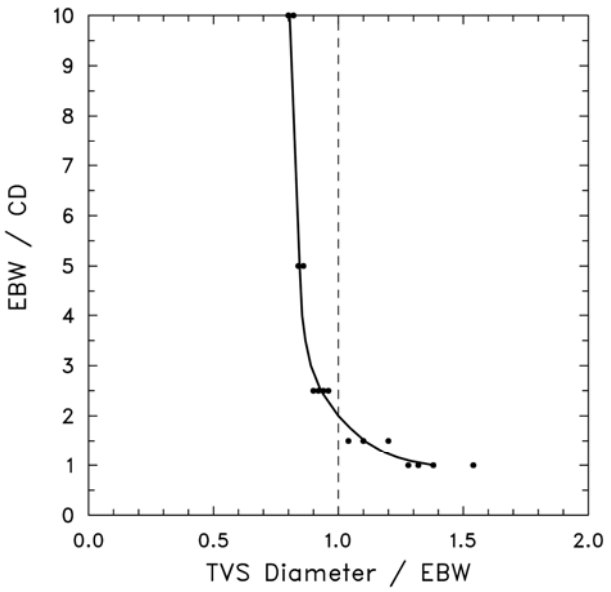

FIG. 4. Distribution of TVS diameter normalized by the effective beamwidth (EBW) as a function of various effective beamwidth to true vortex core diameter (CD) ratios. The dots at a given EBW/CD value represent the four vortex models shown in Fig. 3. The curve represents the mean value of TVS diameter/EBW as a function of EBW/CD. From Wood and Brown (2011).

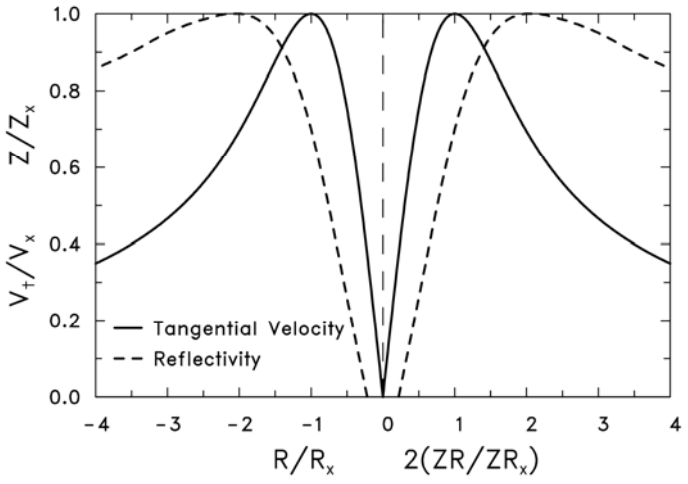

FIG. 5. Relationship of the normalized reflectivity profile (relative to the peak value Z_x) to the normalized Burgers–Rott tangential velocity (relative to the peak value V_x) as a function of radius (ZR, R) from the vortex center normalized by the radius of the respective peak values (ZR_x, R_x).

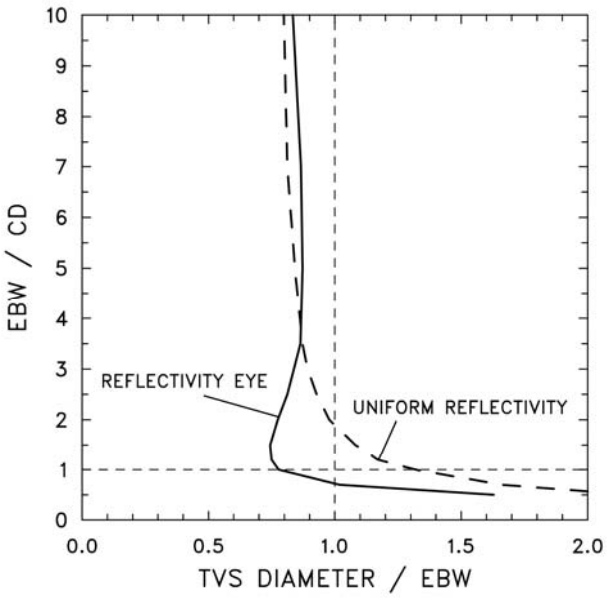

FIG. 6. Simulated TVS diameter relative to the effective beamwidth (EBW) for two reflectivity profiles across a Burgers–Rott vortex as a function of the ratio of the effective beamwidth to the true core diameter (CD) of the vortex. The Doppler velocity signature is defined as a TVS when the effective beamwidth is greater than the core diameter of the vortex (above the horizontal dashed line).